Developmental Cell, Volume *46*

Supplemental Information

Polarity of Neuronal Membrane Traffic Requires Sorting of Kinesin Motor Cargo during Entry into Dendrites by a Microtubule-Associated Septin

Eva P. Karasmanis, Cat-Thi Phan, Dimitrios Angelis, Ilona A. Kesisova, Casper C. Hoogenraad, Richard J. McKenney, and Elias T. Spiliotis

SUPPLEMENTAL FIGURES

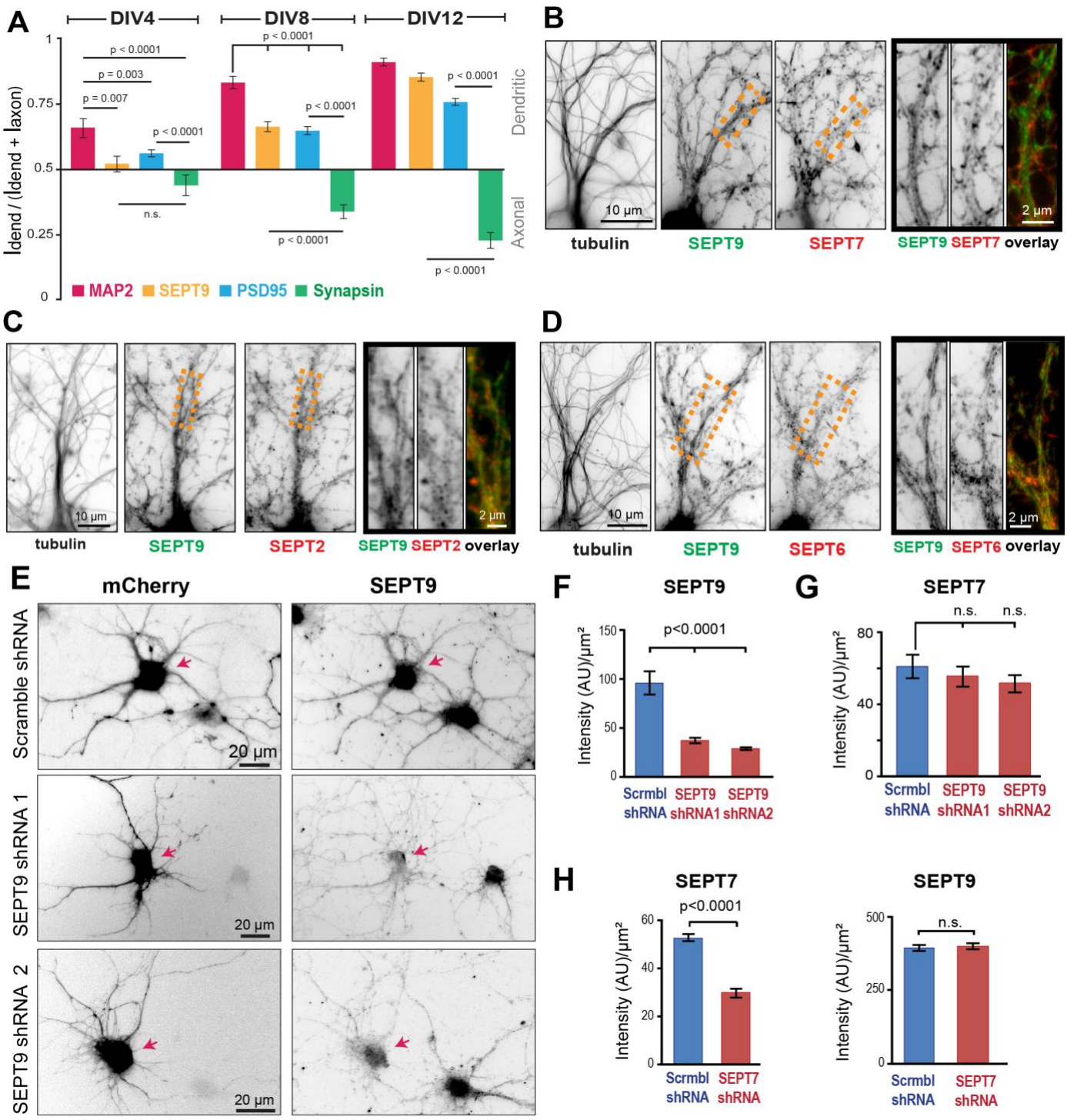

Figure S1. Dendritic enrichment of SEPT9 is concomitant with the establishment of axon-dendrite membrane polarity, and SEPT9 localization to dendrites differs from SEPT2, SEPT6 and SEPT7, Related to Figure 2

(A) Hippocampal neurons were stained at DIV4, DIV8 and DIV12 for endogenous MAP2, SEPT9, PSD95 and synapsin, and fluorescent intensities were quantified in axons and dendrites. The bar graph shows the polarity index – dendritic fluorescence values as a fraction of the sum of dendritic and axonal values for each neuron (n = 20).

(B-D) Images show rat hippocampal neurons (DIV14) stained for MAP2 (not shown), α-tubulin, SEPT9 and SEPT7 (A), SEPT2 (B) or SEPT6 (C). Outlined dendritic areas are shown in higher magnification.

(E-H) Hippocampal neurons (DIV10) were transfected with control and SEPT9 shRNAs (E-G) or SEPT7 shRNA (H) for 48 h, and stained with antibodies against SEPT9 (E-G) and SEPT7 (H). Low resolution wide-field images (E; inverted monochrome) show SEPT9 fluorescence in neurons transfected with vectors that co-express mCherry and scrambled control or SEPT9 shRNAs. Red arrows point to transfected cells. Bar graphs show sum fluorescence intensity per μm^2 (± SEM) per neuronal cell (n = 17-28).

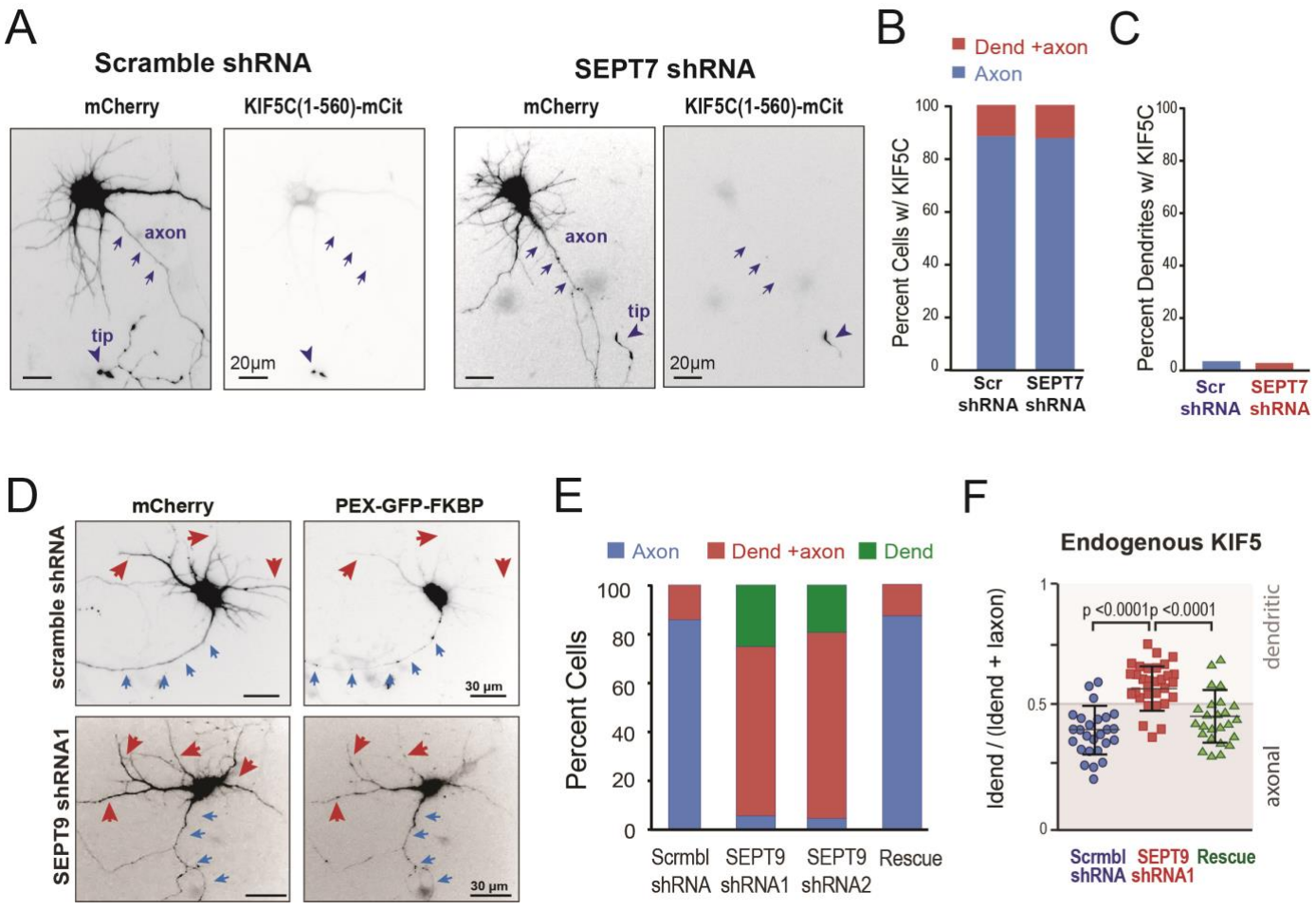

Figure S2. Axonal selectivity of the kinesin-1/KIF5 motor domain requires SEPT9 but not SEPT7, Related to Figure 3

(A-C) Inverted monochrome images (A) show hippocampal neurons that were stained for MAP2 (not shown) after transfection with KIF5C(1-560)-mCit and scramble or SEPT7 shRNAs (mCherry). Blue arrows and arrowheads point to axons and axonal tips, respectively. Bar graphs (B-C) show percent neurons (n = 72-77) with KIF5C(1-560)-mCit in axons or in both axons and dendrites (B), as well as percent of total dendrites (n = 309-503) with KIF5C(1-560)-mCit (C).

(D-E) Hippocampal neurons (DIV10) were transfected with HA-KIF5B(1-807)-FRB, PEX-GFP-FKBP and plasmids that co-expressed scramble or SEPT9 shRNAs with mCherry or shRNA-resistant SEPT9-mCherry (rescue). Neurons were treated with rapalog (2 µM) for 75 minutes. Images (D) show mCherry and PEX-GFP-FKBP in axons (blue arrows) and dendrites (red arrows). Bar graph (E) shows percent neurons (n>60) with PEX-GFP-FKBP in axons only, both axons and dendrites or dendrites only.

(F) Scatter dot plot shows the polarity index of endogenous KIF5 in rat hippocampal neurons transfected with plasmids that co-express scramble (n = 26) or SEPT9 shRNAs (n = 31) with mCherry or shRNA-resistant SEPT9-mCherry (n = 25). Horizontal lines show mean values ± SD.

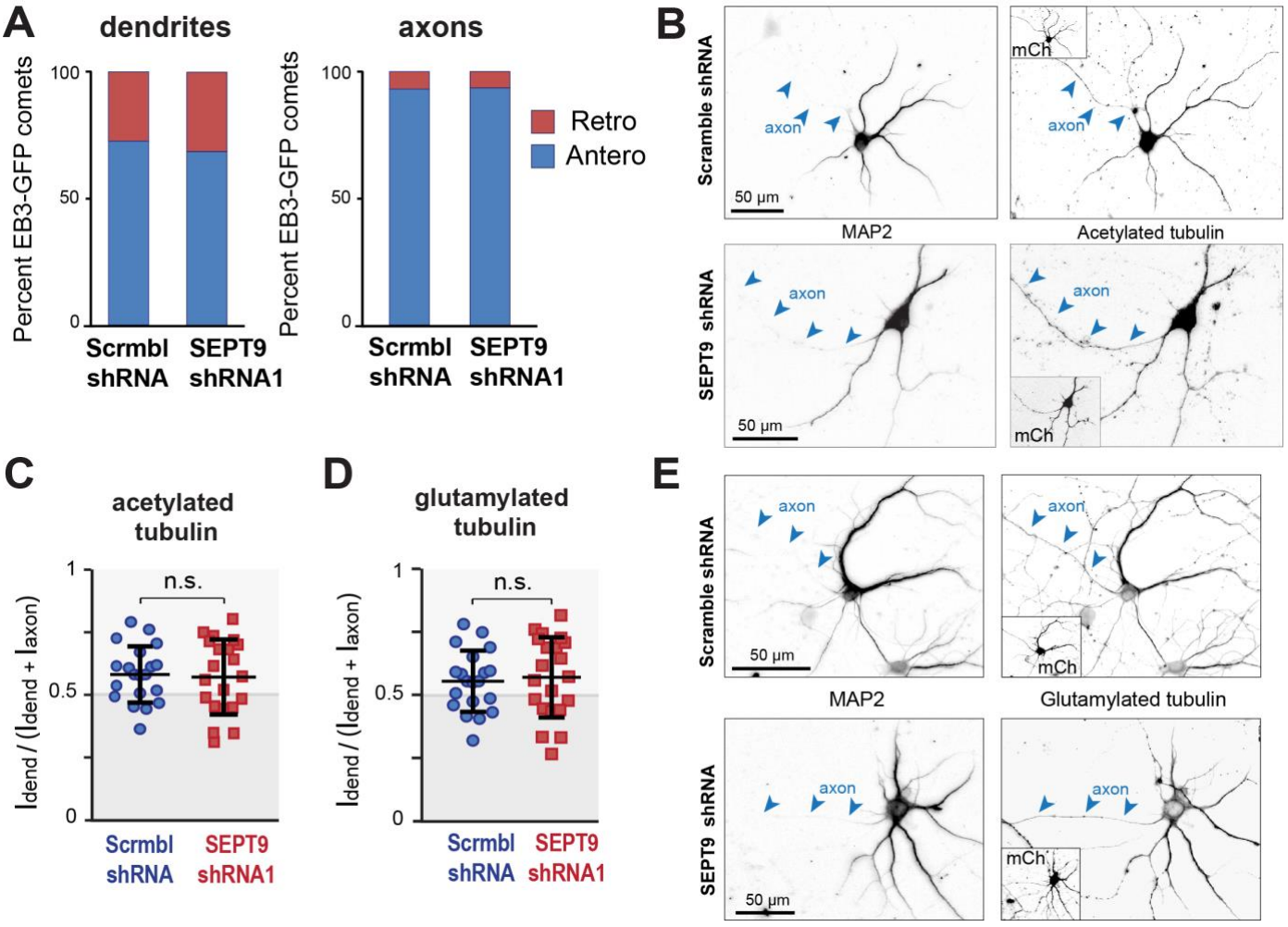

Figure S3: MT orientation, acetylation and glutamylation are not altered in axons-dendrites by SEPT9 depletion, Related to Figure 3 and Figure 5

(A) Hippocampal neurons (DIV10) were co-transfected with EB3-GFP and shRNAs/mCherry for 48 h. Live neurons were stained with an antibody against neurofascin to distinguish axons from dendrites, and EB3-GFP dynamics were imaged with TIRF microscopy. Bar graphs show the quantification of EB3-GFP moving retrogradely and anterogradely in dendrites (n = 275-360 comets; 13 dendrites from 5 cells) or axons (n = 160-180 comets; 6 cells).

(B-C) Wide-field microscopy images (B; inverted monochrome) show hippocampal neurons, which were transfected with shRNAs/mCherry (inset) and stained with antibodies against MAP2 and acetylated tubulin. Scatter dot plots (C) show the ratio of the dendritic fluorescence intensity of acetylated (n = 19-22) tubulin to the sum of their axonal and dendritic intensities. Horizontal lines indicate mean ratios ± SD. Blue arrows point to axons.

(D-E) Wide-field microscopy images (E; inverted monochrome) show hippocampal neurons, which were transfected with shRNAs/mCherry (inset) and stained with antibodies against MAP2 and glutamylated tubulin. Blue arrows point to axons. Scatter dot plots (D) show the ratio of dendritic fluorescence intensity of glutamylated (n = 20-21) tubulin to the sum of their axonal and dendritic intensities. Horizontal lines indicate mean ratios ± SD. Horizontal lines indicate mean ratios ± SD.

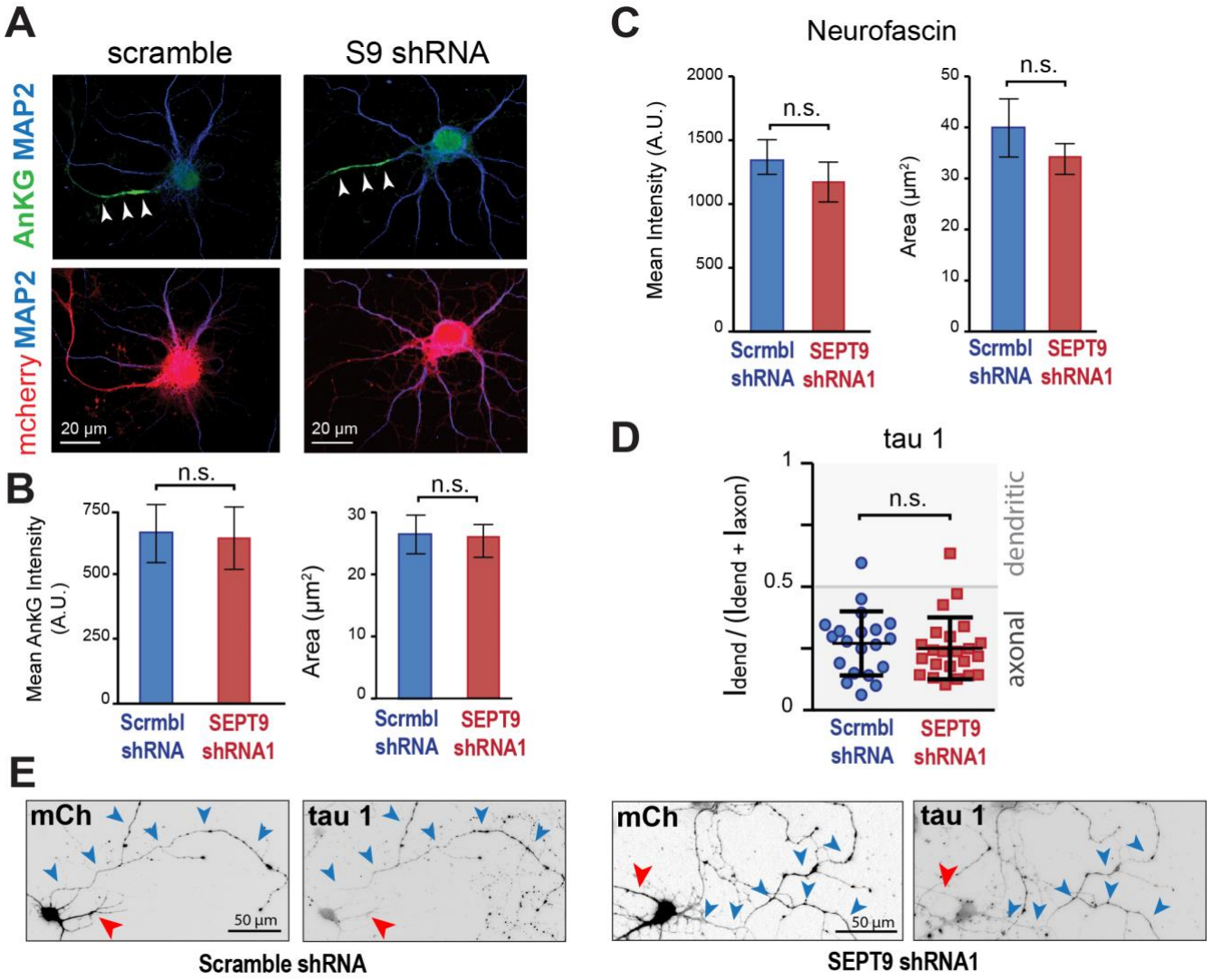

Figure S4: SEPT9 depletion does not disrupt the axonal localization of the AIS markers ankyrin G and neurofascin, or tau, Related to Figure 3

(A) Images show rat hippocampal neurons stained with antibodies against the AIS marker ankyrin-G (green) and MAP2 (blue) after transfection (48 h) with plasmids that co-expressed mCherry (red) and scramble or SEPT9 shRNAs. Arrowheads point to the AIS as outlined by the localization of ankyrin-G.

(B) Bar graphs show the mean (± SEM) fluorescence intensity (left) and surface area (right) of ankyrin G (n = 5 cells).

(C) Bar graphs show the mean (± SEM) fluorescence intensity (left) and surface area (right) of the AIS marker neurofascin (n = 11-16 cells).

(D-E) Scatter dot plot (D) shows the ratio of the dendritic fluorescence intensity of dephosphorylated tau 1 to the sum of its axonal and dendritic intensity in hippocampal neurons (n = 20-23) that were stained for MAP2 after transfection with plasmids expressing mCherry and scramble or control shRNAs. Horizontal lines indicate mean ± SD. Inverted monochrome images (E) of mCherry-expressing (shRNAs) neurons stained for MAP2 and dephosphorylated tau 1. Blue arrows point to axons and red arrows point to dendrites.

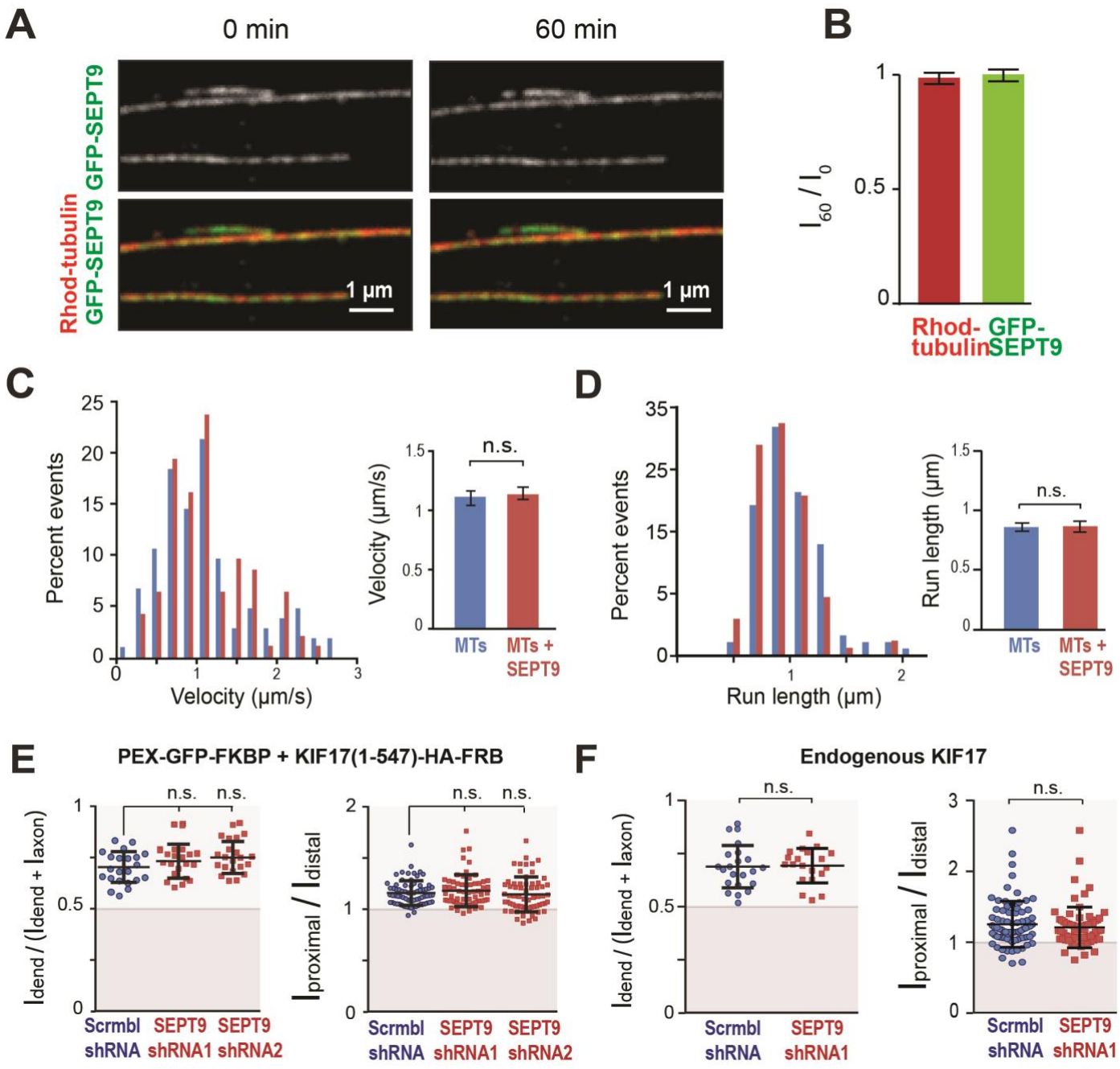

Figure S5: SEPT9 does not affect the motility and localization of kinesin-2/KIF17, Related to Figure 3, Figure 4, Figure 5 and Figure 6

(A-B) Taxol-stabilized rhodamine-labeled MTs were immobilized on glass chambers and incubated with His-GFP-SEPT9 (10 nM). TIRF microscopy images show MTs after 0 and 60 min of washing out all soluble non-bound His-GFP-SEPT9 (A). Bar graph shows the mean fluorescence intensity of rhodamine-tubulin and His-GFP-SEPT9 along MTs (n = 10) at 60 minutes as a fraction of their mean intensities at 0 min (B).

(C-D) Histogram shows the distribution of velocities (C) and run lengths (D) of GFP-KIF17(1-738) on MTs alone (blue; n= 106 events) and MTs coated with 10 nM His-mCherry-SEPT9 (red; n = 98 events). Bar graph shows mean (± SEM) velocity (C) and run length (D).

(E) Hippocampal neurons (DIV10) were transfected for 48 h with PEX-GFP-FKBP, KIF17(1-547)-HA-FRB and control or SEPT9 shRNAs with mCherry. After treatment with rapalog for 105 minutes, cells were fixed and stained for MAP2. Scatter dot plots show ratio of dendritic PEX-GFP-FKBP fluorescence intensity to

sum of its axonal and dendritic intensities (n = 21). Mean fluorescence intensities were also quantified in the proximal and distal halves of dendrites (n = 64-71), and proximal-to-distal ratios were plotted. Horizontal lines indicate mean values ± SD.

(F) Hippocampal neurons were treated with scramble or SEPT9 shRNAs for 48 h, and were stained for endogenous MAP2 and KIF17 after fixation. Scatter dot plots show the ratio of dendritic KIF17 intensity to the sum of its axonal and dendritic intensities (n = 21 cells), and the proximal-to-distal ratio of KIF17 fluorescence intensity in dendrites (n = 71-78).

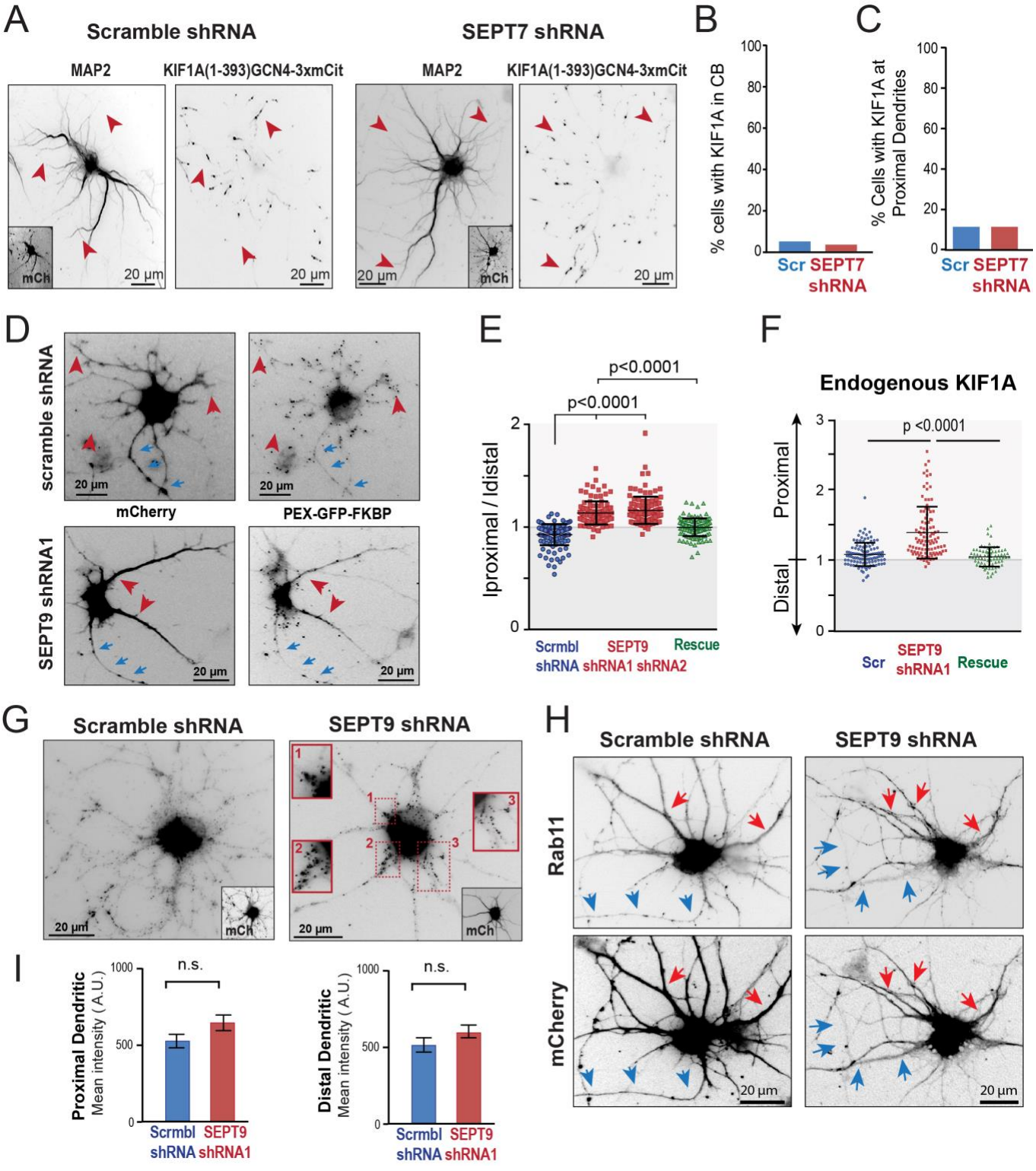

Figure S6: Kinesin-3/KIF1A movement from initial-proximal to distal dendrites requires SEPT9 but not SEPT7, Related to Figure 5

(A-C) Images (A) show DIV12 hippocampal neurons stained for MAP2 after co-transfection with KIF1A (1-393)GCN4-3xmCit and scramble or SEPT7 shRNAs (mCherry; inset). Red arrows point to dendritic tips. Bar graphs (B-C) show percent neurons (n= 56-66) with KIF1A(1-393)GCN4-3xmCit accumulations in their cell body (CB; B) or proximal dendrites (C).

(D-E) Hippocampal neurons (DIV10) were transfected for 48 h with KIF1A(1-489)-HA-FRB, PEX-GFP-FKBP (peroxisomes) and plasmids that co-express scramble/SEPT9 shRNAs and mCherry or shRNA-resistant SEPT9-mCherry (rescue). After treatment with rapalog for 75 minutes, cells were fixed and stained for MAP2 (not shown). Images show mCherry and peroxisomes in axons (blue arrows) and dendrites. Red arrowheads point to peroxisome localization to dendritic tips (scramble shRNA) and along the length of proximal dendrites (SEPT9 shRNA1). Scatter dot plot (E) shows the ratios of proximal to distal dendritic intensities of PEX-GFP-FKBP (n = 25-31 neurons; 108-131 dendrites). Horizontal lines show mean values ± SD.

(F) Scatter dot plot shows the ratios of proximal-to-distal dendritic fluorescence intensities of endogenous KIF1A in rat hippocampal neurons transfected with plasmids that co-express scramble or SEPT9 shRNAs with mCherry or shRNA-resistant SEPT9-mCherry (n = 24-30 neurons; 74-111 dendrites). Horizontal lines show mean values ± SD.

(G) Inverted monochrome images show hippocampal neurons transfected with NPY-GFP and mCherry/shRNAs (inset). Outlined areas show in higher magnification regions of NPY-GFP accumulation at sites of exit from the cell body and proximal dendrites.

(H-I) Inverted monochrome images (H) show hippocampal neurons were transfected with GFP-Rab11 and mCherry/shRNAs and stained for MAP2 (not shown) to identify axons (blue arrows) and dendrites (red arrows). Bar graphs (I) show mean fluorescence intensity (± SEM) of Rab11 in the proximal and distal halves of dendrites (n = 87-91 dendrites; 24 neurons).

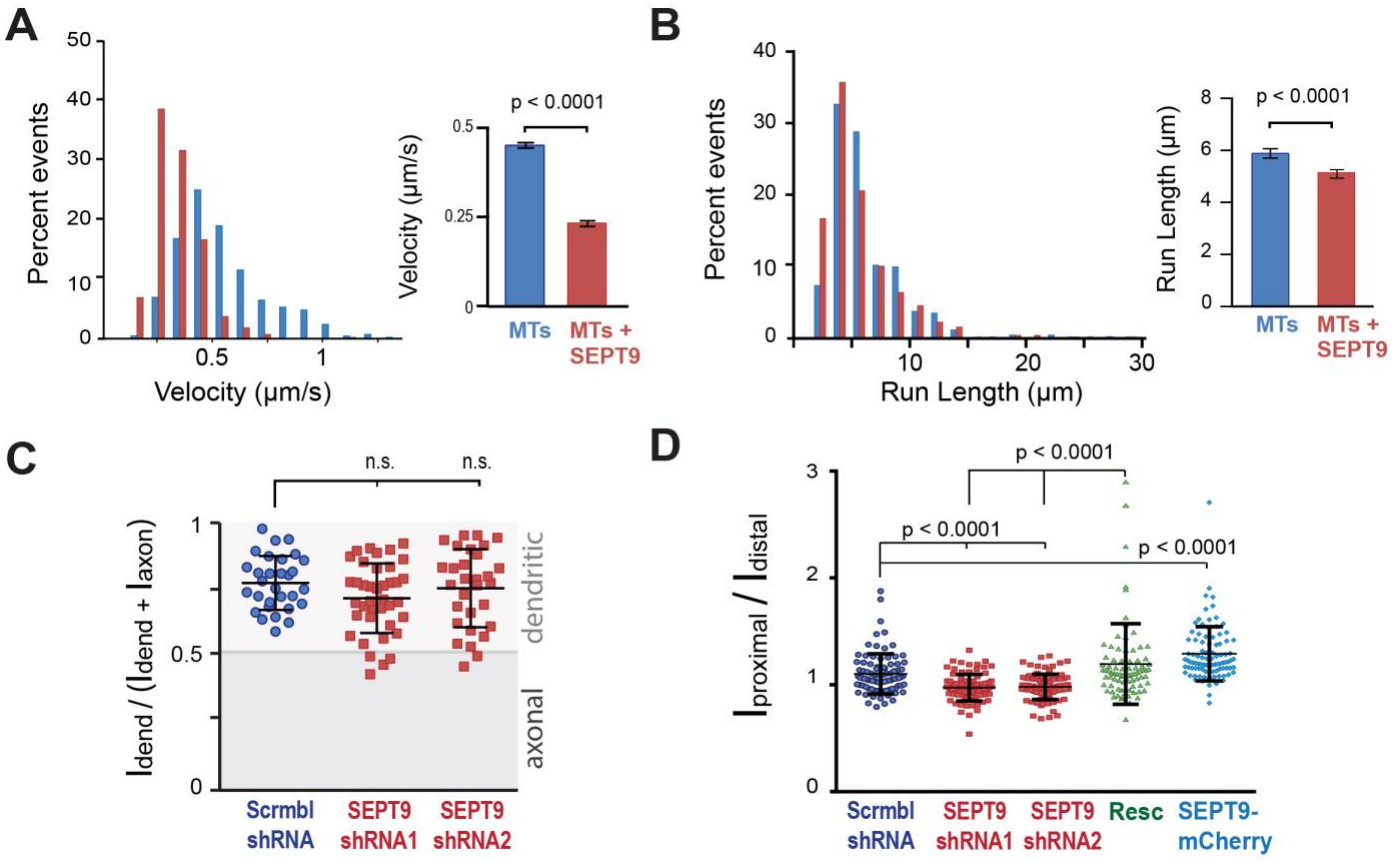

Figure S7: SEPT9 impedes dynein motility in vitro and restricts dynein-driven transport from proximal to distal dendrites, Related to Figure 5 and Figure 6

(A) Histogram shows the distribution of velocities of dynein-dynactin-BicD2 (DDB; n = 418-435) on MTs alone and MTs coated with recombinant His-mCherry-SEPT9 (10 nM). Bar graph shows the mean velocity (± SEM).

(B) Histogram shows the distribution of DDB run lengths and bar graph shows mean run length (± SEM).

(C-D) Hippocampal neurons (DIV10) were transfected with BICDN-FRB, PEX-GFP-FKBP and plasmids that co-express scramble or SEPT9 shRNAs with mCherry (C-D) or shRNA-resistant SEPT9-mCherry (D). Alternatively, BICDN-FRB and PEX-GFP-FKBP were cotransfected and SEPT9-mCherry (D). Neurons were treated with rapalog for 105 min to induce dynein-driven motility of peroxisomes (PEX-GFP-FKBP) and subsequently fixed and stained for MAP2. Scatter dot plot in (C) shows the mean fluorescence intensity of PEX-GFP-FKBP in dendrites as a fraction of the sum of its axonal plus dendritic intensities (n = 30-39 cells). Scatter dot plot in (D) shows the proximal-to-distal ratio of dendritic PEX-GFP-FKBP in neurons where peroxisomes translocated to dendrites. Quantifications were done in neurons with scramble shRNA (n = 89 dendrites; 48 cells), SEPT9 shRNA1 (n = 89 dendrites; 56 cells), SEPT9 shRNA2 (n = 94 dendrites; 30 cells), shRNA1-resistant SEPT9-mCherry (n = 94; 27 cells) or SEPT9-mCherry (n = 94 dendrites; 26 cells). Horizontal lines show mean values ± SD.